Progress toward a complete metrology set for the International X-ray Observatory (IXO) soft x-ray mirrors

J. P. Lehan,[a,b] M. Atanossova,[b,c] K.-W. Chan,[a,b], T. Hadjimichael,[b,d]
T.T. Saha,[b] M. Hong,[b,e] W. W. Zhang,[b] and P. Blake[b]

[a]Center for Research and Exploration in Space Science and Technology, NASA Goddard Space Flight Center, and Department of Physics, University of Maryland, Baltimore County, 1000 Hilltop Circle, Baltimore, Maryland 21250
[b]NASA Goddard Space Flight Center, Greenbelt, Maryland 20771
[c]Oak Ridge Associated Universities, MC100-44, P.O. Box 117,Oak Ridge, TN 37831
[d]Ball Aerospace, 1616 McCormick Drive, Upper Marlboro, MD 20774
[e]SGT, Inc, 7701 Greenbelt Road, Suite 400,Greenbelt, MD 20770

ABSTRACT

We present an overview update of the metrologic approach to be employed for the segmented mirror fabrication for the IXO soft x-ray telescope. We compare results achieved to date with mission requirements. This is discussed in terms of inherent capability versus in-practice capability of the metrology. We find that all the needed metrology equipment are in hand but that a number of the needed quantities remain too uncertain relative to mission requirements. This is driven by the mounting of the mirrors themselves. We then discuss some plans for addressing the mirror mounting issues. Finally, we also briefly discuss some promising mandrel metrology techniques.

Keywords: Optical metrology, x-ray optics, IXO

1.0 INTRODUCTION

1.1 IXO & the Soft X-ray Telescope overview

The International X-ray Observatory (IXO)[1,2,3,4] is an international x-ray astrophysics mission to be flown in 2020 as a follow-on to the current Chandra and XMM Newton observatories. By combining a much higher effective area, good spatial resolution, and greater spectral resolving power at the Iron K lines, this observatory will be a powerful tool for observing more-distant black holes, investigating dark matter, and elucidating galactic evolution.

The mission concept consists of a single spacecraft with one 3.3 m diameter, 20 m focal length, 5 arc-sec HPD soft x-ray telescope with 361 nested, azimuthally segmented shells of grazing incidence mirrors. In the configuration discussed here, the primary/secondary shells are approximately 0.4 mm thick and segmented azimuthally to reduce the mirror size. The substrate material is glass (Schott D263) coated with iridium. Details of the segment fabrication are described elsewhere.[4] The telescope is divided into 60 modules (each with many nested primary/secondary reflector pairs) to ease assembly. A portion of the telescope field of view will be available for dispersive spectroscopy. In addition, the focal plane will have a CCD array for imaging, a microcalorimeter array for x-ray nondispersive spectroscopy, a polarimeter and a host of other instruments. See reference 1 for a complete mission description.

1.2 Metrology requirements for the segmented x-ray mirrors

The metrology requirements are based on the mission error budget. Table 1 lists the preliminary mirror segment error budget along with the metrology accuracy needed to determine those requirements. The old versus new error budget terms represent the shift in requirements from the Constellation-X (spectroscopy-based) mission to the IXO mission. Thus this paper to large extent concentrates on how the methods developed for the Constellation-X mission perform

Optics for EUV, X-Ray, and Gamma-Ray Astronomy IV, edited by Stephen L. O'Dell, Giovanni Pareschi, Proc. of SPIE Vol. 7437, 74370R · © 2009 SPIE
CCC code: 0277-786X/09/$18 · doi: 10.1117/12.826625

relative to the new requirements for IXO and, if appropriate, means of achieving the needed improvements.

Table 1: Summary of the preliminary IX0 mirror error budget allocations and the metrology requirements needed to determine them. Note that the metrologic requirements are expressed as one standard deviation expected from a single measurement. The roll-up of the mirror error terms results in a 4 arc-sec HPD for the primary-secondary pair at the image plane. [Based on November 2008 mission error budget.]

Error Term	Old Budgeted Error	New Budgeted Error	Metrologic Requirement	Current Metrology Method
Average Radius	100 μm	4 μm	1 μm	CCMM
Average Cone Angle	30 arc-sec	1.19 arc-sec	0.4 arc-sec	Hartmann[1] /Null Lens
Radius error	5 μm RMS	0.2 μm RMS	0.07 μm RMS	Hartmann/ Null Lens
ΔΔR (Cone Angle Variation)	0.5 μm RMS	0.67 arc-sec RMS	0.22 arc-sec RMS	Hartmann/ Null Lens
Average Axial Sag	0.31 μm P-V[5]	0.24 μm RMS	0.08 μm RMS	Null Lens
Axial Sag Variation	0.11 μm P-V	0.26 μm RMS	0.09 μm RMS	Null Lens
Low frequency errors[2]	2.4 arc-sec RMS[6]	20.3 nm RMS	6.8 nm RMS	Null Lens
Mid-frequency errors[3]	- - -	2.8 nm RMS	1.0 nm RMS	Null Lens
Microroughness[4]	0.5 nm,RMS	0.5 nm,RMS	0.2 nm,RMS	Mireau Interferometry

[1]The Hartmann test measures focal length so we must combine with the CCMM radius to calculate the cone angle
[2]Axial errors in the spatial period range from 200-20 mm after removal of 2nd order (sag)
[3]Axial errors in the spatial period range from 20-2 mm
[4]Microroughness defined here to be over the spatial period range from 2 mm to 1 μm
[5]Previous error budget expressed this term in um, we express them here in these units to be consistent with the previous publication
[6]Previous error budget grouped low and mid-frequencies and was expressed as a slope error rather than the directly measurable RMS height error – see also not #5

1.3 Instrumental versus in-practice performance

For the thin glass mirrors, the measurement accuracy never reaches the accuracy inherent to the instrument. This can be separated into two primary causes fundamental to the problem: self weight deformation and vibration. In a previous publication,[5] we addressed both of these issues and concluded that the vibration is adequately being managed for most of the measurements. The self-weight distortion, although better managed than at that time, continues to limit the metrology accuracy and repeatability, especially in light of the stricter requirements.

Table 2: Summary of the preliminary metrology error budget requirements and the metrology uncertainties obtained to date. Note these in-practice uncertainties include (and are dominated by) the mirror fixturing.

Error Term	Metrology Uncertainty Allowable	Metrology Method	In-Practice Uncertainty[3]	Notes
Average Radius	1 μm	CCMM	20 μm	1
Average Cone Angle	0.6 arc-sec	Hartmann	5 arc-sec	1
Radius error	0.1 μm RMS	Hartmann/ Null Lens	0.5/0.06 μm RMS	1/1
ΔΔR (Cone Angle Variation)	0.3 arc-sec RMS	Hartmann/ Null Lens	0.3/0.13 arc-sec RMS	1/1
Average Axial Sag	0.12 μm RMS	Null Lens	0.005 μm RMS	1
Axial Sag Variation	0.13 μm RMS	Null Lens	0.03 μm RMS	1
Low-frequency errors	6.8 nm RMS	Null Lens	20 nm RMS	1
Mid-frequency errors	1.0 nm RMS	Null Lens	1.2 nm RMS	2
Microroughness	0.2 nm,RMS	Mireau Interferometer	0.2 nm RMS	2

1. Variation dominated by mounting repeatability
2. Uncertainty not dominated by mounting
3. Uncertainty as expressed here is related to the ability to measure the same part at two separate times and get the same answer and was determined from repeatability tests performed at different intervals on a few representative mirrors.

For our thin mirrors, the self-weight deformations exceed the metrology instrument uncertainties for the low spatial frequency band of the measurements. Thus, discussion of the mirror shape independent of its mount is meaningless. We will talk about mounting in association with the measurements that employ the mount. Table 2 shows the error budget terms, metrology method used to measure them, and the in-practice metrology uncertainty achieved to date. The in-practice uncertainty includes the influence of the self-weight deformation for most of the error budget terms.

2. METROLOGY METHODS

2.1 Grazing-incidence Hartmann Test

We have discussed this method previously but outline it here briefly for completeness. The Hartmann test is well known in near-normal-incidence optics,[6] but at grazing incidence, the mirror shrinks to essentially a single circular zone of constant radius. So a grazing-incidence Hartmann test samples the entire radial extent of the mirror but only a very small portion azimuthally.

The primary improvements in this method have come in the mounting. The self-leveling spring mount has been replaced by a hard suspension mount.[7] This mounting is much stiffer resulting in reduced deformations under gravity. The optical beam employed for the Hartmann test travels horizontally which is not the minimum-distortion orientation for the mirrors. A periscoped version of the Hartmann test is under construction that will allow the mirror to be measured vertically which should yield more accurate measurements. This should also provide excellent agreement with the measurements performed by the null lens (§2.3) since the orientations will be the same.

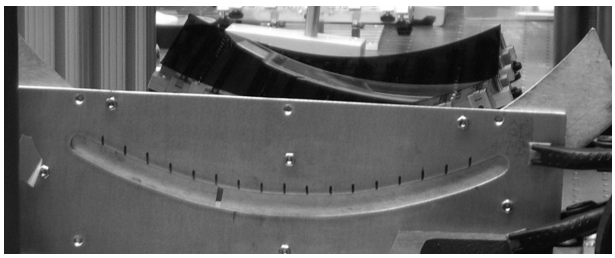

Figure 1: Grazing-incidence Hartmann mask (foreground) and mirror under test (dark object in middle ground). The mask is moved sequentially to the 15 positions marked and the resultant centroid positions determined. [After ref. 5]

In addition to its metrology function, the Hartmann set-up is used for evaluating potential flight-mount-induced mirror distortions and in pre-alignment of the secondary mirror to the primary mirror prior to x-ray beam testing.

2.2 Cylindrical coordinate measuring machine (CCMM)

We have reported on this method previously[5] so provide only the briefest summary here. We employ a custom designed non-contact coordinate measuring machine in a cylindrical geometry for determination of the large-scale geometry of the mirrors (Figure 2). This CMM employs a confocal optical probe developed by Stil SA. Our version uses Stil's highest sensitivity probe, with a quoted RMS distance uncertainty of approximately 2 nm and about 20 microns total accessible range. It employs precision stages for radial position, vertical position, and azimuthal position with a measured radial noise of about 40 nm RMS. This is less than the goal for the instrument but still exceeding most other commercial non-contact probes.

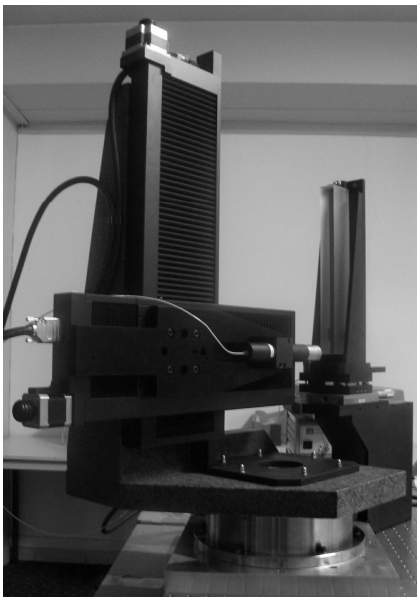

Figure 2: Non-contact Cylindrical Coordinate Measuring Machine (CCMM). The optical probe is attached to precision rotation, radial and z linear stages. The calibration flat is shown on the right but the part under test is not shown in this photograph. [After ref. 5]

The performance of the system is limited in practice by three factors: mirror vibration, mirror alignment stage movement, and thermal drift. The latter two factors are a result of the measurement time required for adequate sampling of an entire mirror. Each point requires sufficient samples to average over the vibrations at that point. Thus, the measurement of an entire mirror takes several hours to complete. In principle, the instrument can measure almost all of the mirror parameters in Table 2. To accomplish this to the needed precision, however, the drift allowable in the stages and mounts is only tens of nm over the measurement time. In addition, the thermal stability needs to be of the same order over a similar timeframe. We have not been able to achieve the combination of mount and thermal stability to measure all parameters with the required precision. In addition, the very long measurement times prevent consideration of this technique for mirror metrology during the flight telescope build. Currently, however, it is the preferred method for determining mirror average radius. We plan on eliminating it as new methods based on the null lens (§2.3) and Hartmann test (§2.1) are commissioned in the coming year.

2.3 Refractive null lens and strobe Fizeau interferometer

The combination of a refractive null lens and strobe interferometer covers the figure of the mirrors in the spatial period band from 200 mm to 2 mm. This normal incidence metrologic technique enables a much greater spatial fidelity of the mirror surface than practical with the grazing-incidence Hartmann technique or CCMM. Although the null lens is compatible with any commercial Fizeau interferometer with a sufficiently large collimated beam (>225 mm diameter here), we employ a 4D Technologies FizCam1500® with a 250 mm aperture. This strobe interferometer typically operates at a 0.2 msec staring time and a frame rate of 15 frames per second when performing our measurements. This limits the sampling of vibrational frequencies to only 7.5 Hz so only the lowest mirror vibrational mode is Nyquist sampled. Thus, we rely on random impulses and the law of large numbers to yield a representative average shape. Figure 3 illustrates the null lens and strobe Fizeau in use.

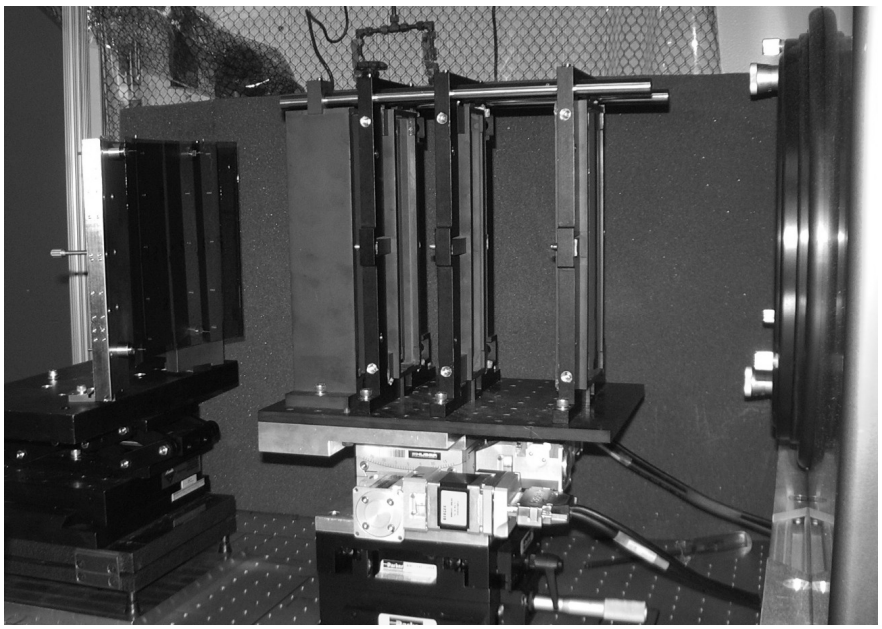

Figure 3: 60 degree field-of-view cylindrical null lens and strobe Fizeau interferometer measuring mirror. Interferometer is to the far right (in the foreground); the (4-element) cylindrical null lens is in the center, and the mirror under test (in the suspension mount) is on the left.

The null lens is cylindrical in geometry and is of a newer design[8] than reported in 2007. It consists of 4 air-spaced elements (see Fig. 3) and can measure a mirror of up to 60 degree azimuthal span and 215 mm axial extent. This allows an entire IXO mirror to be measured in a single measurement. In addition to the reduced measurement time over the previous lens, the low-order mirror figure is more accurately determined because stitching is not required. Also, the ability to measure an entire part at once enables more terms in the error budget to be determined with the null lens. Specifically, these are the average cone angle and radius.

One difficulty in interferometric characterization of very thin mirrors is uniqueness. That is, the shapes resultant from misalignments can also be valid (error and distortion) shapes for the parts themselves. This is not unique to thin mirrors but the normal method of rectifying this type of ambiguity is measuring the part in multiple orientations as is typical for absolute testing. This proves problematic for very thin mirrors because the gravity distortions change the part shape significantly as the part is manipulated in a gravity field. To ameliorate the ambiguity of a single measurement we measure it several times with small known alignment perturbations between measurements. This is accomplished by small movements of the null lens rather than the mirror. This assures that the mirror shape is definitely the same between measurements and only alignment has changed. A simultaneous fit of the multiple interferograms then yields a unique solution for the shape of the mirror in most cases.

The use of a null lens has an advantage over other methods like diffractive optics because only a single lens is needed for the entire telescope since tilting the lens relative to the interferometer beam creates a beam that is a good approximation to a cone. Also, reasonably large distortions can be accommodated allowing mounting distortions to be investigated quantitatively.

The calibration of the null lens proves critical to achieving the needed accuracy for the IXO mission (Table 1). The speed of the new null lens and its virtual focus make calibration somewhat more difficult than the previous version. A scanned (sampled) calibration has been performed but a full surface calibration requires a large precision concave cylindrical reference mirror. Such a reference can be made by diamond turning and is being procured. The lowest order error in such a diamond-turned mirror of concern for calibration is the cone angle. This residual cone angle is readily deduced with our Hartmann set-up.

Because the entire bandwidth of the interferometer is needed to determine the performance relative to the error budget of Table 1, the interferometric set-up also needs to be calibrated as a function of spatial frequency. This can be approached in two manners. The first is a two-step operation that treats the interferometer as a black box. The first step is to characterize the interferometer as outlined in reference 9 using a specially-designed reference mirror. This allows an effective optical transfer function of the interferometer to be constructed. Then the optical transfer function of the null lens can be convolved with the response of the interferometer. Alternatively, a better method is to have a full optical model of the test set-up which includes the interferometer. This allows a spatial frequency correction to be applied to the data as a function of the null lens field of view, interferometer zoom, etc. This correction is most important for the mid-frequency slope errors of Table 1 where imperfect imaging in the null-lens-interferometer optical train becomes apparent.

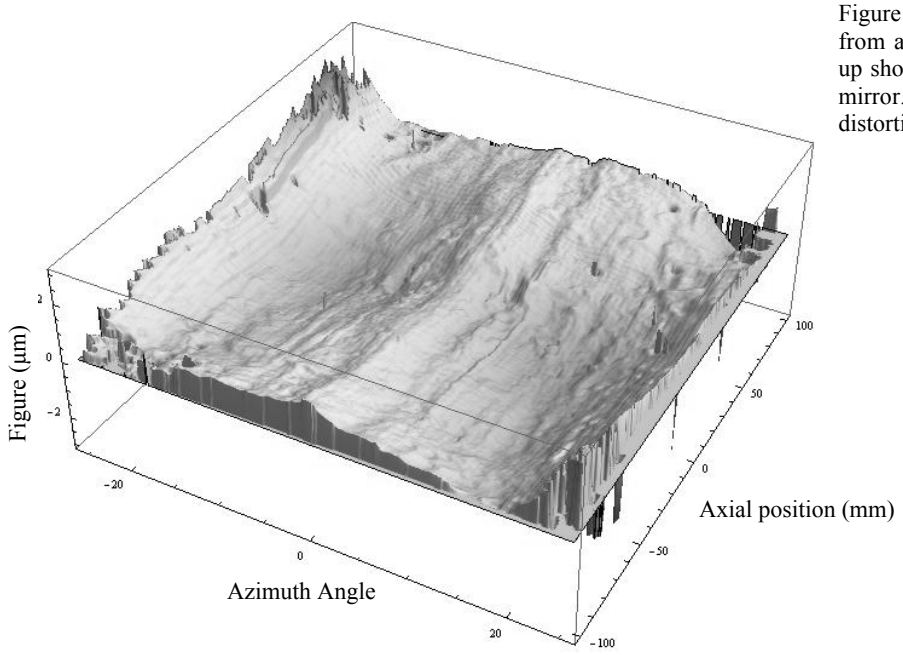

Figure 4: Typical surface map (deviation from a cone) obtained from the null lens set-up shown in Fig. 3 for a 50-degree secondary mirror. This map includes the gravity distortions induced by the mounting.

The gravity distortion is the dominant impediment preventing the gravity-free shape of the mirrors from being determined and is governed by the fixturing. We employ two approaches to mounting for interferometry. The first is the semi-kinematic "suspension mount"[7] seen in Fig. 3. This mounting scheme is semi-permanent in that small amounts of adhesive hold the mirror to posts situated near the minimum deflection points. Once mounted, the measurements have good repeatability. On the other hand, repeated mountings of the same mirror do not reliably result in the same mirror shape to within the tolerance needed for the mission at this time. The second mount is the so-called "Cantor-Tree" mount.[5,10] This mount is also semi-kinematic and is akin to a 1-dimensional whiffle-tree with a mirror-image "upper branch" whiffle-tree that bears almost none of the mirror load but does suppress vibration. This mount is free of adhesives but suffers from frictional forces that limit its degree-of-repeatability with consecutive mountings of the same mirror. Currently, neither mounting system's repeatability is yet adequate for the needs of IXO. A reduced-friction Cantor Tree mount (Fig. 5) is being fabricated which should improve the mount repeatability to an acceptable level. The suspension mount, too, is undergoing continuous improvements and will ultimately be limited by the local distortions at the bond points. This is acceptable if they represent a small enough areal fraction of the segment.

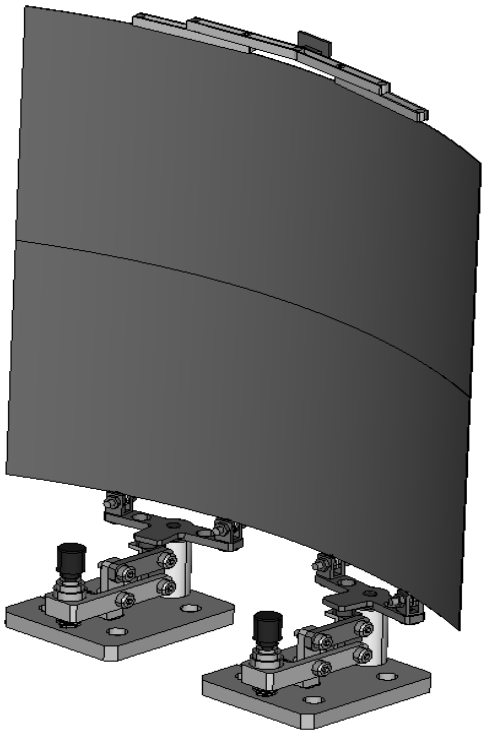

Figure 5: Cantor Tree mount with minimal friction-induced distortion. The lower branches have v-grooved bearings that mate to the mirror edge so that the mirror can move freely as it compresses in the gravity field. These, in turn, swivel in the orthogonal plane and each branch also swivels to match the two-point slope of the mirror's edge. The black knobs allow each lower branch of the Cantor Tree to be raised or lowered so that the load on each lower branch is equal. This is measured by small load cells (not apparent in the picture). The upper branch of the Cantor Tree has all the same rotational degrees of freedom as the lower branch with the exception of the v-grooved bearings which are not needed since the mirror can slide readily along its edge at the top.

2.4 Mireau interferometry

We have reported on this method previously[5] and no modifications to the method have been needed in the intervening time so we limit our discussion here. We employ a Mireau interferometer to measure the mirrors at spatial periods 2 mm to 1 μm. We employ two models (a Zygo NewView® and an ADE Phase Shift MicroXam®). The gravity distortions appear only as tilt in this spatial period band so fixturing is not difficult. Performance of both instruments is comparable and we are regularly achieving the performance expected from the manufacturers' specifications.

2.5 Mandrel Metrology

With the advent of the IXO mission, the requirements on mandrels for the mission have increased significantly. Whereas the dimensional and roughness specifications are easily within the capabilities of modern optical fabrication technology, the metrology is non-standard for most optical fabrication facilities. Preliminary mandrel specifications based upon the mirror error budget of Table 1 are presented in Table 3. Of note is that the microroughness is not important for the precision glass slumping discussed here because this spatial frequency portion of the mandrel figure

does not transfer to the glass substrates during forming. This is very unlike other x-ray replication techniques where super-polishing of the mandrels is often required.

There are two aspects to the mandrel metrology problem that make it particularly challenging. The first is the spatial bandwidth over which metrology data is needed. For the mandrels this is 0.003 - 1 mm^{-1}. The second challenge is timing. To meet the delivery schedule for the mission, about one mandrel per day needs to be yielded. This requires either a large number of parallel lines or rapid *in situ* metrology. We have been pursuing two general technologies that hold promise to address both the spatial frequency and throughput challenges.

The first is just an adaptation of the null lens technology currently employed with the mirrors. For the mandrels, the requirements of the mount are greatly relaxed given the part stiffness. Thus the null lens method becomes very repeatable. The addition of a precision tip-tilt stage to a radius bench allows the local radius and cone angle (over the field of view of the lens) to be determined. By stitching sub-apertures together, a full 3D map can be determined to good accuracy. The advantage of this a technique is that it is universal. That is, one set-up can measure any of the mandrels.

The second method is a one-shot metrology method that would allow the entire active area of the mandrel to be measured with two computer-generated holograms (CGH's).[11] The advantage of this method is that almost the entire compliment of mandrel parameters are determined simultaneously and registered to each other. The disadvantages are the sizes, and the numbers of CGH's required for the mission.

Table 3 also compares the two proposed methods for a single sub-aperture exposure. Both methods are limited by their field of view but the mandrel lens gains a portion of this back by performing a local radius measurement using the radius slide. In practice the precision and accuracy of this radius measurement will be limited by the stage movements in three-space. (Note: The dual CGH method could employ the perturbation method discussed in §2.3 to improve its performance but this was not one of the assumptions included in the comparison of Table 3.)

For smaller mandrels, the dual-CGH method can perform the measurement in one exposure reducing the measurement time considerably. The null lens will require stitching for these mandrels, increasing the measurement time in comparison with the dual-CGH method. For the larger mandrels, both methods will require stitching the data because neither large enough lenses nor CGH's are practical at this time.

Table 3: Summary of a proposed IXO mandrel metrology error budget and estimates for the metrology methods being pursued. This table addresses only repeatability expectations, not accuracy, so the table implicitly assumes the calibration error is a negligible fraction of the overall error.

Error Term	**Mirror Budgeted Error**	**Mandrel Budgeted Error**	**Null Lens Estimated Uncertainty[2,3]**	**Dual-CGH Estimated Uncertainty[2,4]**
Average Radius	4 μm	2 μm	0.5 μm	2 μm
Average Cone Angle	1.19 arc-sec	0.6 arc-sec	0.5 arc-sec	0.2 arc-sec
Radius error	0.2 μm RMS	0.1 μm RMS	0.1 μm RMS	0.07 μm RMS
ΔΔR (Cone Angle Variation)	0.67 arc-sec RMS	0.3 arc-sec RMS	0.1 arc-sec RMS	0.1 arc-sec RMS
Average Axial Sag	0.24 μm RMS	0.12 μm RMS	0.001 μm RMS	0.002 μm RMS
Axial Sag Variation	0.26 μm RMS	0.13 μm RMS	0.002 μm RMS	0.004 μm RMS
Low frequency errors	20.3 nm RMS	10.2 nm RMS	1.5 nm RMS	2 nm RMS
Mid-frequency errors	2.8 nm RMS	1.4 nm RMS	2 nm RMS[1]	2 nm RMS[1]
Microroughness	0.5 nm RMS	NA	NA	NA

[1]Needs interferometer spatial frequency calibration
[2]Uncertainty here is only repeatability rather than the accuracy which is implied by the mandrel error budget as well
[3]Assumes radius bench with 0.1 μm precision, 0.1 arc-sec tilt stage, and orthogonal distance measuring interferometers for a single exposure with a 15º FOV
[4]Single exposure of 140 mm aperture prototype optics with a 27º FOV

2.5 Optical performance predictions

Though not a metrology technique, mathematical modeling to predict the expected x-ray performance is an important

aspect of our metrology plan. The good agreement seen between the modeled performance and previous x-ray measurements has allowed us to gain confidence in the model's ability to predict this performance and our metrology on which the model is based. This, in turn, allows us to measure much fewer mirrors in the x-ray saving considerable time and labor.

For the modeling, we calculate the point spread function (PSF) of a measured mirror pair from the diffraction integral given, for example, in reference 12 (Eqs. 3.488, 3,489, and 3.490). Since the axial errors are dominant in grazing incidence systems, we calculate the wave front error and PSF in the radial planes only, and then incoherently add the PSF's in the focal plane of a large number of such planes at a variety of azimuths. The wavefront error is calculated over all relevant spatial frequencies from the lowest order figure error of the mirrors to the micro-roughness of the mirrors (see Table 1).

Depending on the metrology mount employed, this will provide either a mirror ranking (or approximate ground performance prediction) or an accurate assessment of the ground test performance. The use of the suspension mount allows the mirror to move all the way through metrology and into x-ray testing and has helped verify the model as well as given us increased confidence in our metrology measurements.

3. CONCLUSIONS

We presented the error budget terms and associated metrologic goals for the IXO mission. We also presented the current metrology used to meet the particular requirements for those terms on these ultra-lightweight segmented glass x-ray optics. The increased mission requirements are challenging the metrology in a variety of areas. Whereas the inherent capabilities of the metrology methods are able to achieve these goals, the nature of the thin mirrors continues to thwart attempts to determine the mirror shapes to the needed accuracy. Further gains in metrology will be driven by improvements in holding the mirrors for measurement. When a mirror can be mounted and remounted and the same shape deduced, then finite element modeling can calculate the needed zero-gravity shape. This goal has so far eluded us but improvements in both the Cantor Tree Mount and Suspension Mounting hold promise for the future.

ACKNOWLEDGEMENTS

This work is funded through the IXO technology development program. This work represents the contributions of numerous people beyond the author list. In particular we wish to acknowledge our collaborators at NIST, Drs. Gaugjun Gao, Ulf Griesmann, and Johannes Soons for their tireless efforts on the dual-CGH method and Ms. Linnette Kolos for technical support. We also want to thank Mr. Raymond Russell for providing the Cantor Tree drawing. Mention of trade names or commercial products does not constitute endorsement or recommendation by the authors or NASA.

REFERENCES

[1] For an overview, see the description of IXO online at http://ixo.gsfc.nasa.gov/

[2] Robinson, D. and R. McClelland," Mechanical Overview of the International X-Ray Observatory**,**" IEEE Aerospace Conference, IEEEAC paper #1580 (2009).

[3] McClelland, R., and D. Robinson, "Design Concept for the International X-Ray Observatory Flight Mirror Assembly," IEEE Aerospace Conference, IEEEAC paper #1574 (2009).

[4] Zhang, W. W., et al, "Mirror technology development for the International X-Ray Observatory (IXO) mission," Proc. SPIE. **7360**, 73600J (2009).

[5] Lehan, J. P., S. Owens, T. Hadjimichael, M. Hong, K.-W. Chan, T. T. Saha, P. Reid, and W. W. Zhang, “Toward a complete metrologic solution for the mirrors for the Constellation-X Spectroscopy x-ray telescope,” Proc. SPIE **6688** 668818 (2007).

[6] I. Ghozeil in *Optical Shop Testing*, D. Malacara (ed.),Wiley, New York, pp.323-349 (1978).

[7] Chan, K.-W., W. W. Zhang, T. Saha, J. P. Lehan, J. Mazzarella, L. Lozipone, M. Hong, and G. Byron, "Opto-mechanics of the Constellation-X SXT mirrors: challenges in mounting and assembling the mirror segments ", Proc. SPIE **7011**, 701114-1-9 (2008).

[8] Lehan, J. P., G. Byron, R. McClelland, T. Hadjimichael, R. Russell and D. Robinson, "An alignment procedure for multi-element precision cylinder lenses and modular enclosure to house them," Proc. SPIE **7433**, 7433-7-1-8 (2009).

[9] Chu, J., Q. Wang, J. P. Lehan, G. Gao, and U. Griesmann, "Measuring the phase transfer function of a phase-shifting interferometer," Proc. SPIE **7064** 70640C (2008).

[10] Lehan, J. P., T. Saha, W. W. Zhang, S. Owens Rohrbach, K.-W. Chan, T. Hadjimichael, M. Hong, and W. Davis, "Some considerations for precision metrology of thin x-ray mirrors," Proc. SPIE **7018** 701815-1 -8 (2008).

[11] Gao, G., J. P. Lehan, W. Zhang, U. Griesmann, and J. Soons, "Computer-generated hologram cavity interferometry test for large x-ray mirror mandrels: design," Opt. Eng. **48**(6) 063602 (2009).

[12] Wilson, R. N., *Reflecting Telescope Optics*, Springer-Verlag, Berlin (2000).